Tellus (1985), *37B*, 259–271

Terrain-induced effects on the ozone, temperature and water vapour daily variation in the upper part of the PBL over hilly terrain

By B. BRODER* and H. A. GYGAX**, *Atmospheric Physics ETH, Hönggerberg, CH-8093 Zürich, Switzerland*

(Manuscript received December 28, 1984; in final form May 20, 1985)

ABSTRACT

Measurements of the daily variation of several meteorological and chemical parameters in the planetary boundary layer above the crest-height of a mountain-valley system of the Swiss Plateau are presented. On the basis of the observations, it is concluded that processes at the earth-atmosphere boundary are contributing strongly to the ozone losses, the increase in humidity, and the cooling rates observed during night-time at these higher levels. Surface-layer effects are coupled to the upper part of the boundary layer by transport processes, which result from the orographic forcing of the mean wind field (i.e. occurrence of the phenomenon of blocking) and the interaction of mean flow with locally-induced wind systems. Thus the observations cannot be interpreted purely by local effects. In this part of the planetary boundary layer, the additional influence of processes due to the complex topography on a more regional scale is also felt. It is stressed that this coupling should be adequately represented in atmospheric pollution models of non-homogeneous terrain.

1. Introduction

To assess the air quality of the environment and establish air pollution control strategies, it is necessary to obtain a thorough understanding of the chemical as well as dynamical processes occurring within the planetary boundary layer (PBL). A large number of studies of these processes and their coupling has been undertaken for homogeneous terrain. However, for non-homogeneous terrain only few results from field-experiments and model-studies are available.

For such terrain, it is particularly known that blocking is a significant and important phenomenon. Blocking, i.e., the existence of stagnant air masses below the crest line of a mountain-valley system, may occur, if the Froude-number drops below a certain critical value. The Froude-number Fr is defined as follows:

$$\mathrm{Fr} = \bar{u}/N \cdot H, \tag{1}$$

where $\bar{u}$ is the mean wind speed above the ridge line, H indicates the crest height and N is the Brunt-Vaisala frequency (cf. Manins and Sawford, 1982). Bell and Thompson (1980) infer from their laboratory-experiments and numerical studies a critical Froude-number of 1.3, whereas from Manins and Sawford (1982) a critical limit of 1.6 is given. If the conditions for the occurrence of blocking are met, one can assume that the lower part of the PBL is much more influenced by local processes than the layers above the ridge line. Furthermore a drastic change in the wind field structure is expected if stagnant air masses form (Bell and Thompson, 1980).

The aim of the present study is to examine the effects of this specific flow feature and the related transport processes on the physico-chemical structure of the PBL layers above the ridge line of a mountain-valley system.

* Present affiliation: Cantonal Laboratory, Air Quality Section, Frohbergstrasse 3, CH-9000 St. Gallen, Switzerland.

** Present affiliation: Cantonal Office of Environmental Protection, Air Quality Section, Route des Cliniques 17, CH-1700 Fribourg, Switzerland.

2. Measurements

2.1. Measurement program and techniques

The field work was conducted in the Reuss valley, a flat bottomed valley on the Swiss Plateau near Zürich. Ground stations, equipped for measurements of ozone, temperature, wind and light intensity, were set up at the following sites: Grod (G, 410 m above the ground level of the valley floor (AGL)); Herdmatten (H, 120 m AGL); Merenschwand (M, 0 m AGL); Schüren (S, 150 m AGL) and Aeugst (A, 350 m AGL). These lay roughly along a line perpendicular to the axis of the valley through Merenschwand (Figs. 1, 2 and 3). NO/NO_x-measurements were made at Grod, Merenschwand and Aeugst. In addition, vertical profiles of ozone, temperature, wind and humidity up to about 800 m AGL were determined at Merenschwand and Schüren by means of tethered balloons. A "grab" sampling instrument was used at Merenschwand for measuring the NO_x content at predetermined levels within the PBL. Finally, free balloon ascents yielded ozone, temperature and humidity data up to the mid-troposphere. The ground stations were operated continuously and some 14 tethered balloon soundings per day were carried out at Merenschwand and Schüren. The vertical distribution of the NO_x content was determined by 2 to 4 ascents, and 1 to 2 free balloon flights were conducted per day. With the exception of the "grab" sampling technique which is discussed elsewhere (Gygax et al., 1985), data collection methods were conventional.

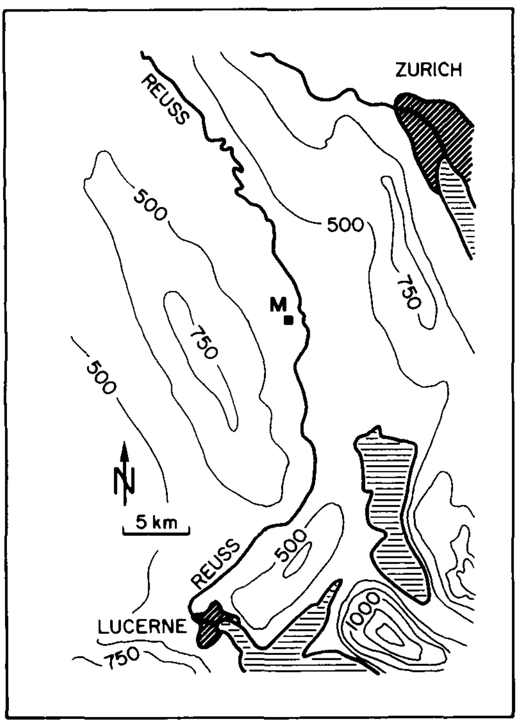

Fig. 1. Map of the Reuss valley. M indicates the position of the measuring site Merenschwand. (Heights are in meters above sea level.)

On the slopes of the Reuss valley, the ground is covered with grass, brushwood and woodland, whereas at the bottom of the valley agriculture is mainly important with products like maize, strawberries and potatoes.

2.2. Data selection

Days with full-time measurements were classified and only taken into consideration if a stable weather period over 24 h was encountered, weak synoptic winds and a defined local wind system could be observed and no night-time ozone concentration exceeding the daytime values occurred (i.e., no simple evidence for advective influence related to ozone was recognized). Moreover for the remaining 14 days, an analysis of the Berlin weather chart 850 mb indicated that temperature and humidity did not show a strong influence of large-scale advection. From these days, four averaging periods were chosen considering seasonal factors (Table 1). This procedure served to isolate the effects of fog and the changing time of sunrise. In the late summer, one period was chosen on the basis of very high NO/NO_x concentrations (period 4).

3. Results

During our measurements, the conditions for the occurrence of blocking were met during all nights. This can be concluded by comparing the computed values for the Froude-number (Appendix A) with the critical limit of 1.3 given by Manins and Sawford (1982) as well as from the fact that the local wind system was clearly in evidence against the background of synoptic scale winds (Broder and Gygax, 1985). From the discussion of the phenomenon of blocking in Section 1, it seems

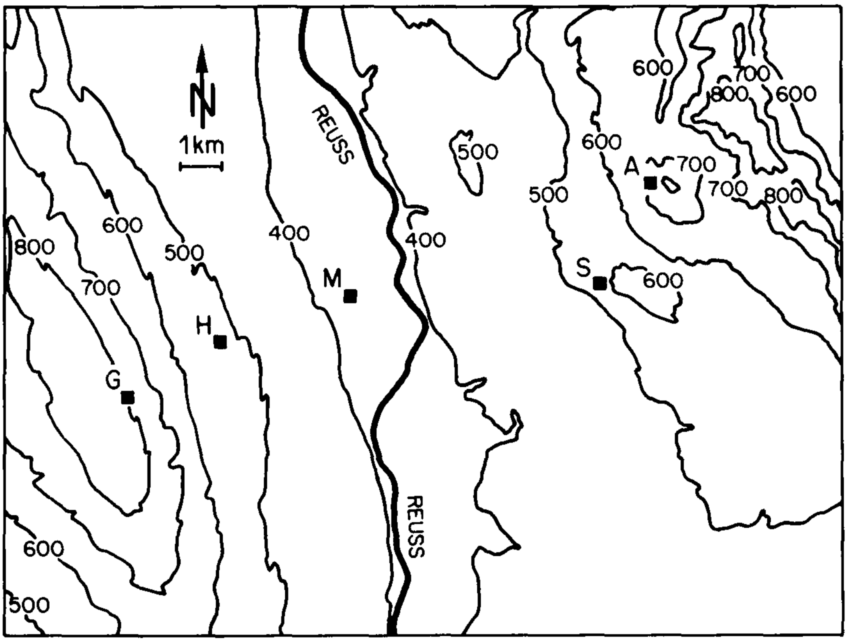

Fig. 2. Part of the map of the Reuss valley. Positions of the ground stations are indicated by G: Grod, H: Herdmatten, M: Merenschwand, S: Schüren and A: Aeugst. (Heights are in meters.)

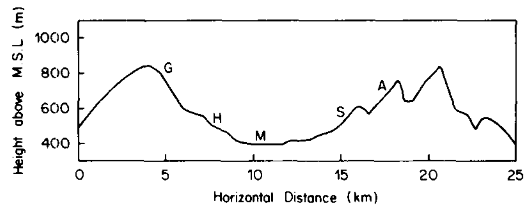

Fig. 3. Vertical cross section through the Reuss valley at Merenschwand with indicated positions of ground stations.

reasonable to analyze the data from the layers below and above the ridge line separately. Although this paper deals mainly with the upper part, for a better understanding, a brief description of the results from the analysis in the layers 0–400 m is given.

3.1. *Structure of the lower part of the PBL*

Measurements at the ground show that the daily maxima in temperature and ozone mixing ratio are very well correlated in magnitude. From this fact and considering the temperature dependency of the smog reactions, it can be inferred that smog photochemistry strongly influences the air at the measurement site. Moreover the air within the boundary layer often shows higher ozone mixing ratios compared with the air in the free troposphere. The existence of these ozone-rich layers further confirms the significant contribution of smog photochemistry within all parts of the PBL (Figs. 4 and 5).

For the lower part of the PBL, a statistical analysis was undertaken of the rate of ozone loss at night. The results were presented in a recent publication of the authors (Broder and Gygax, 1985) and will only briefly be summarized here. It is concluded that homogeneous chemistry accounts on average for 19% (extreme values were 4% and 54%) of the observed ozone destruction rates. The main effect is due to the reaction between nitric oxide and ozone. The remaining ozone destruction is attributable to the dry deposition of ozone at the surface. From a comparison with other related studies, it is concluded that during the night-time regime this process is much more effective in the hilly terrain around the measuring site than over horizontally homogeneous terrain. This increase in efficiency cannot be explained by direct vertical

Table 1. *Ozone mixing ratio, potential temperature, water vapour mixing ratio, given as average values for the 400–800 m height interval at 1800 LST and 0600 LST respectively, difference (D) between both values and quadrant of wind direction in the same height interval at 1800 LST and 0600 LST*

	Days	Ozone			Potential temperature			Humidity			Wind direction	
		ppb			K-273		K	g/kg			quadrant	
Averaging period	1982	18	06	*D*	18	06	*D*	18	06	*D*	18	06
1 (no fog)	25/26 May	62	46	−16	19.3	17.7	−1.5	6.3	6.4	+0.1	N–E	E–S
	1/2 June	81	63	−18	27.3	20.8	−6.5	7.8	9.8	+2.0	N–E	W–N
	2/3 June	89	68	−21	27.1	21.5	−5.6	7.4	8.5	+1.1	W–N	W–N
	3/4 June	100	73	−27	27.7	22.7	−5.0	7.8	9.4	+1.6	N–E	W–N
2 (with fog)	21/22 Aug.	48	35	−13	17.7	14.8	−2.9	6.5	6.6	+0.1	W–N	N–E
	22/23 Aug.	65	45	−20	19.4	17.1	−2.3	5.8	7.2	+1.4	W–N	S–W
	29/30 Aug.	55	37	−18	20.0	17.0	−3.0	8.8	9.2	+0.4	N–E	S–W
3 (with fog)	3/4 Sept.	61	49	−12	21.3	19.4	−1.9	9.3	10.0	+0.7	N–E	S–W
	4/5 Sept.	66	49	−17	27.5	24.6	−2.9	9.9	10.0	+0.1	W–N	S–W
	9/10 Sept.	62	45	−17	21.4	19.4	−2.0	9.9	10.7	+0.8	N–E	S–W
	11/12 Sept.	93	49	−44	24.6	20.8	−3.8	10.9	11.3	+0.4	N–E	N–E
4 (with fog)	10/11 Sept.	79	54	−25	24.1	21.7	−2.4	9.5	11.8	+2.3	N–E	S–W
	12/13 Sept.	69	57	−12	24.4	21.2	−3.2	9.1	11.9	+2.8	N–E	N–E
	13/14 Sept.	74	52	−22	23.9	20.5	−3.4	9.3	10.1	+0.8	N–E	N–E

Data are from Merenschwand, height is in meters above valley ground (m AGL); LST: Local Summer Time, i.e. GMT – 2 hours; Wind direction: N: North, E: East, S: South, W: West.

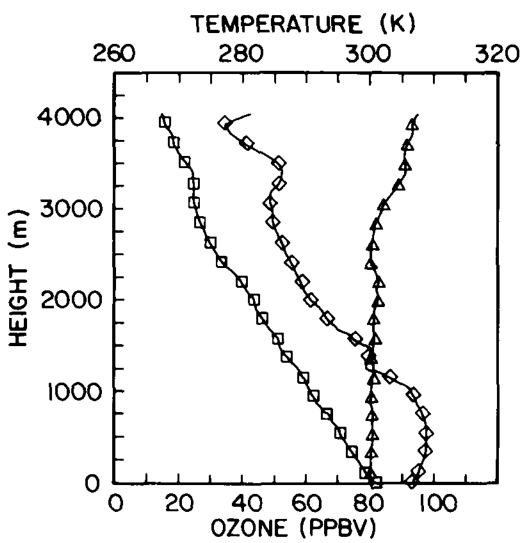

Fig. 4. Free balloon ascent data of 3 June 1982. (Merenschwand: 1653 LST). Symbols: □: temperature, △: potential temperature and ◇: ozone.

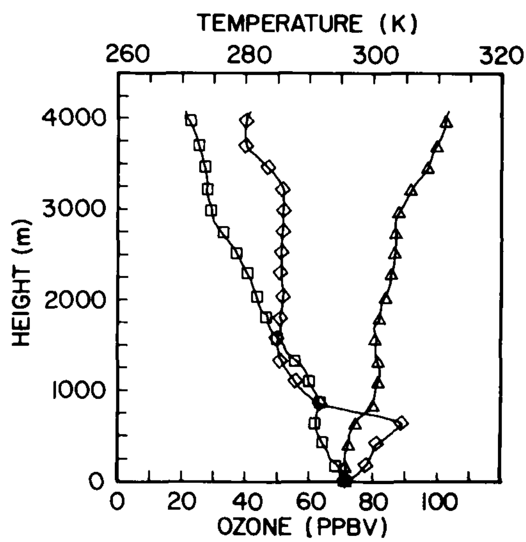

Fig. 5. Free balloon ascent data of 10 September 1982. (Merenschwand: 1700 LST). Symbols see Fig. 4.

turbulent transport, since only absolutely unrealistic turbulent exchange coefficients in the surface layer above the valley bottom together with extremely high deposition velocities for ozone would result in the observed ozone destruction rates. It is concluded that this increase in efficiency of ozone deposition is linked to the influence of a local cross-valley wind system. The occurrence and structure of this system are deduced from the measurements of several meteorological parameters (in particular wind speed and direction). The ozone destruction due to dry deposition occurs mainly in regions of night-time downslope winds and hence the air reaching the bottom of the valley has a very low ozone content. It follows that the upward airflow associated with this local wind system (typical vertical wind speed of the order of 1 cm/s) gives rise to the observed continuous ozone depletion within the lower part of the boundary layer.

3.2 Structure of PBL height-interval 400–800 m

In the upper part of the PBL, no occurrence of blocked air masses is to be expected. Thus it must be assumed that the influence of local effects will be very different to that below the ridge line.

This is particularly the case for the upward motion, which occurs due to the existence of a local induced cross-valley wind system. Assuming a somewhat large vertical wind speed of 2 cm/s (to compare with the wind speeds consistent with the ozone loss rates in the lower part of the PBL of the order of 1 cm/s), it would take 5.5 h for the air in the height interval 400–800 m to be replaced by air from the layer between the ground and 400 m. However, during this time the air masses have drifted away by some 40 km (typical horizontal wind speed is of the order of 2 m/s). In consequence, only the air in a layer just above the ridge height (mean vertical thickness of 80 m) will be influenced by the air masses transported by the local wind system (valley width ~16 km). Thus horizontal advective transport processes may be important for the structure of this part of the PBL, and a great variability in the behaviour of the meteorological parameters and trace gas concentrations might be expected. But Table 1 shows that for the night-time budgets of the different parameters within the layer of 400–800 m, very clear tendencies are evident (see also Figs. 6 and 7).

3.2.1. Effects due to large-scale horizontal transport and turbulent exchange

Naturally it might be possible to explain the observed variations by the influence of large-scale horizontal advection not recognized by analysing the weather charts (cf. Subsection 2.2). But in this case, one would expect at least some days out of 14 to show a decrease in the water vapour content within the layers under consideration. This is not observed. Additionally no indications exist that our observations might be due to the regularity in the occurrence of advective transport processes during our measuring periods, since a great variety of wind direction changes was observed (Table 1). Furthermore, no substantial differences occur in the night-time budgets of ozone, temperature and humidity between the days with winds from constant directions and those with varying wind quadrants. For the days with constant wind direction, an ozone decrease of 20 ppb, a temperature loss of 4 K and an increase in the humidity content of 1.3 g/kg can be computed from Table 1. The other days show mean values for the ozone loss of 18 ppb, temperature decrease of 3 K and increase in humidity of 0.95 g/kg.

On the basis of these statistical arguments, we thus conclude that in addition to large scale horizontal transport, other processes must occur which give rise to the definite night-time trends observed within the layer of 400–800 m. However, the measured short time variations (time scale of the order of 2 to 4 h) must be fully attributed to horizontal advective transport, since our measurements show that fully developed turbulence occurs not after 2100 LST (critical limit for the Richardson-number: 0.25; see Appendix B), and intermittent turbulence activity is only possible in period 3 before midnight. This latter conclusion is drawn on the basis of the computed Ri-numbers (Appendix B) using a criterion given by Kondo et al. (1978): these authors report that intermittent turbulence may exist if the values of the Richardson-number Ri are between approx. 0.25 and 1.0. From our observations, it can also be inferred that between 2000 LST and 0600 LST, for 85% of the time, Ri exceeds the value of 1.0, i.e, the critical limit for occurrence of any turbulence (Appendix B). This is clearly due to the very stable stratification and the almost vanishing vertical gradients of wind velocity within this upper layer (Figs. 6 and 7). Thus, we additionally conclude that as in the

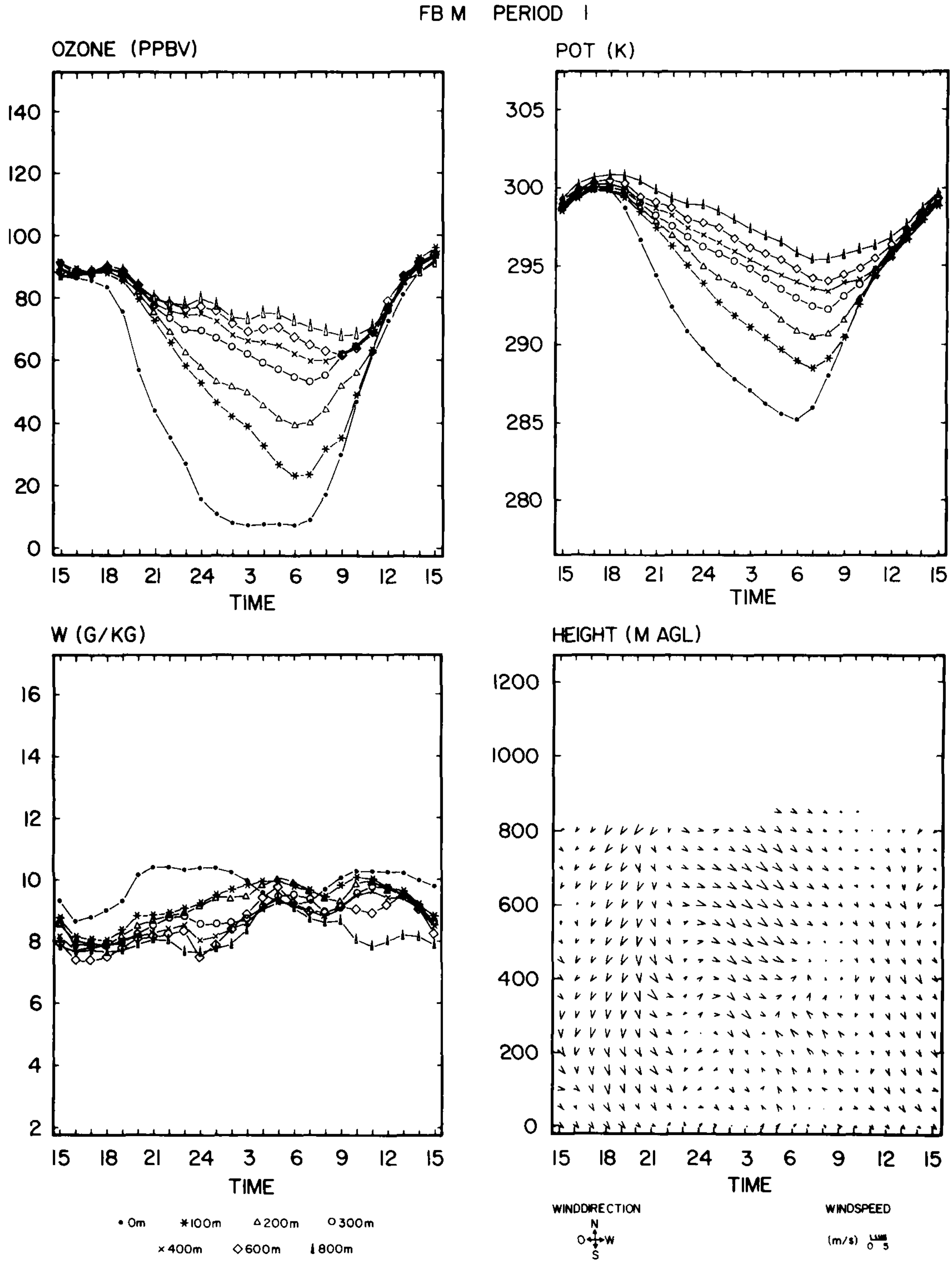

Fig. 6. Tethered balloon data from Merenschwand for period 1. Parameters: ozone, potential temperature (POT, reference level is 0 m AGL), water vapour mixing ratio (W) and wind as vector-arrows. (Height is in m AGL.)

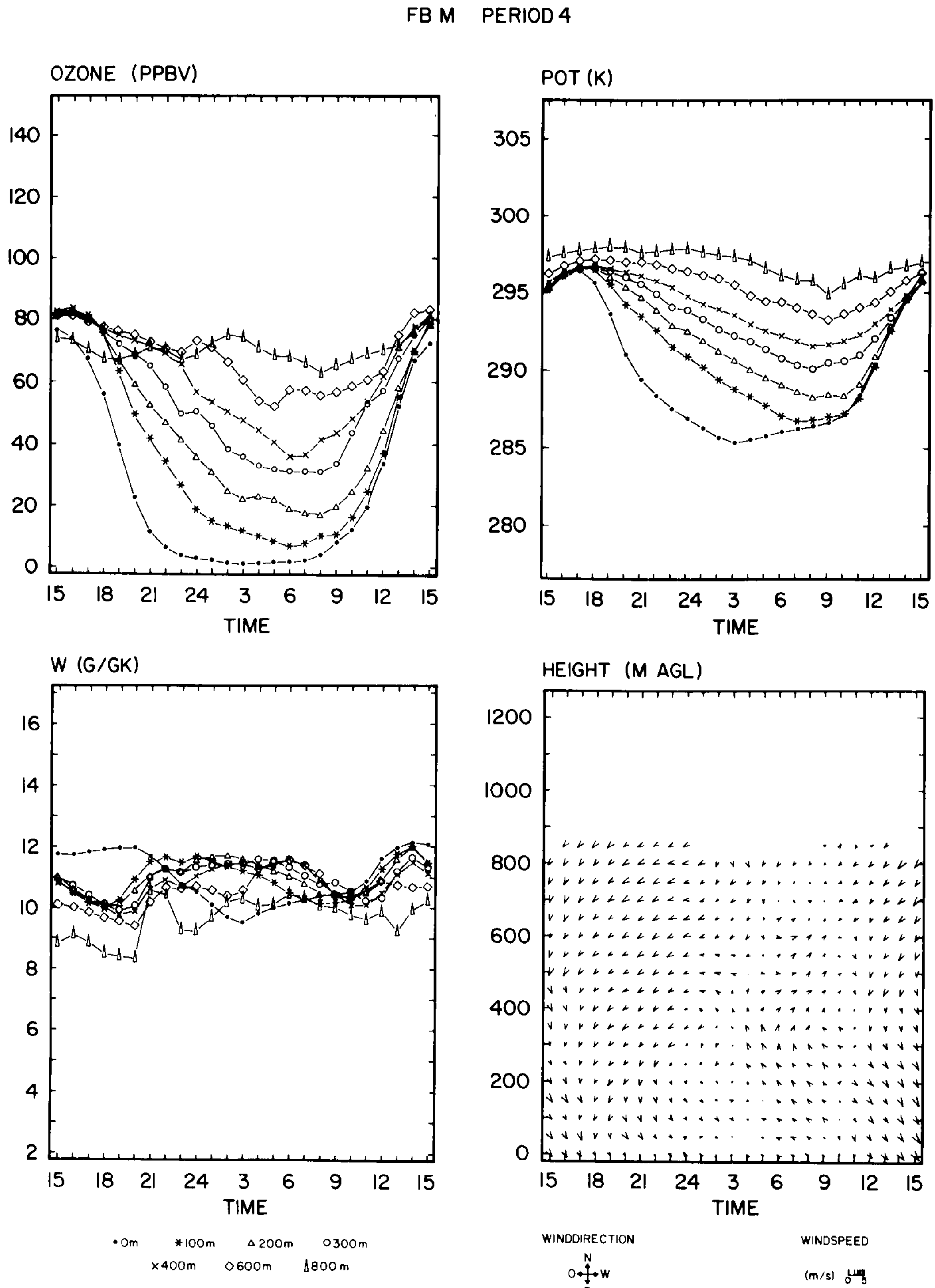

Fig. 7. Tethered balloon data from Merenschwand for period 4. Parameters as in Fig. 6.

lower part of the PBL (cf. Subsection 3.1) turbulent transport proves ineffective in the layers under consideration.

Thus, neither large-scale horizontal transport nor turbulent exchange is mainly responsible for the observed trends in the variation of the ozone mixing ratio, temperature and humidity content.

3.2.2. Processes in isolated air masses

The following discussions are intended to clarify the rôle of processes occurring in the air masses which are assumed to be isolated from the surroundings, i.e., no coupling by transport exists with the layers below or above. The most important of these processes are homogeneous chemistry (acting as a sink for ozone) and radiational cooling (giving rise to a temperature decrease).

3.2.2.1. Ozone. The implication is that no NO_X is transported from the ground to the upper levels. This seems reasonable to assume, since turbulent transport is very ineffective during night-time, as discussed above. The observations show that during our measuring periods, NO_X mixing ratios in the order of 5 ppb occurred in the layers above the crest height and no significant change in the NO_X content was observed during night-time (Fig. 8). At these levels, NO_X exists mainly in the form of NO_2 due to the reaction between NO and O_3:

$$NO + O_3 \rightarrow NO_2 + O_2. \qquad (R1)$$

NO_2 can react fairly fast with O_3 according to R2:

$$NO_2 + O_3 \rightarrow NO_3 + O_2. \qquad (R2)$$

Thus, it is expected that the NO_2 content drops to 0 and an ozone loss of 5 ppb is observed during night-time, since no efficient reactions exist to rebuild NO and NO_2 from the products of R_2 and following reactions (Platt et al., 1981). However, no decrease in the NO_2 content is observed, whereas the ozone loss is much higher than expected. Two explanations for this behaviour seem possible:

(1) Some as yet unknown reactions exist, which rebuild NO and NO_2 from the products of R2 and following reactions (e.g. N_2O_5).
(2) Since it is most likely that our NO_X measuring devices show an interference with NO_3 and N_2O_5, the NO_2 decrease cannot be detected. Since peroxyacetylnitrate (PAN) and other trace constituents are measured as NO_X, the late evening NO_2 mixing ratio is overestimated as well (Broder and Gygax, 1985; Gygax et al., 1985).

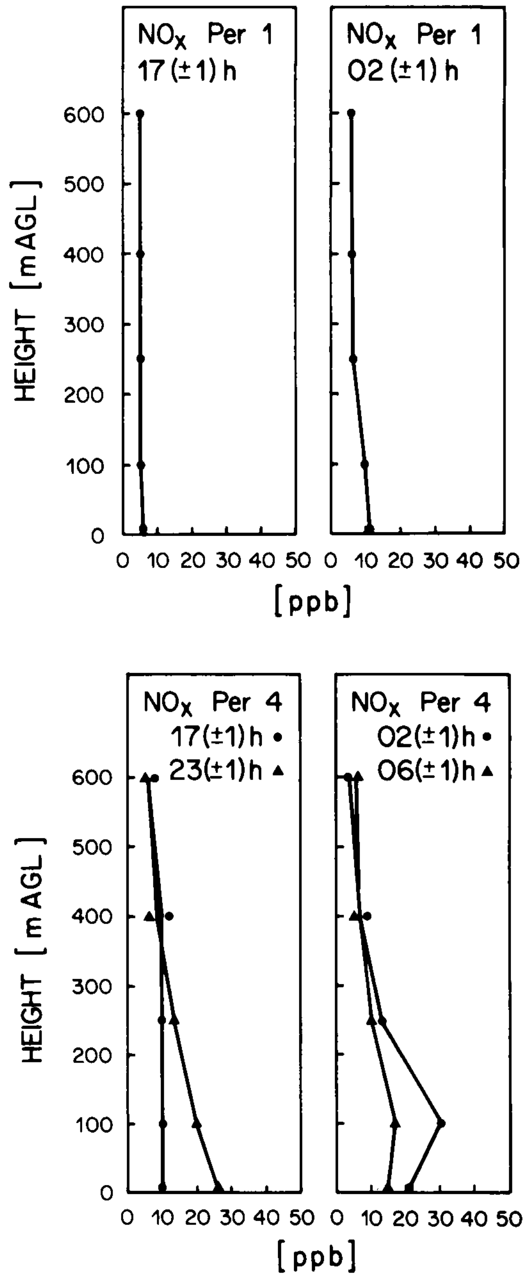

Fig. 8. Vertical profiles of NO_X at different times of day for Merenschwand during periods 1 and 4. (Height is in m AGL).

If the first explanation would be true, a large amount of the night-time ozone loss rate could be explained by the effects of homogeneous chemical processes. However, from the analysis of the ozone destruction rates in the lower part of the PBL, it can be concluded that this explanation is not compatible with our observations (Broder and Gygax, 1985). Thus we reject this assumption. The consequence of the second explanation is that the ozone loss due to homogeneous chemistry is overestimated if a value of 5 ppb is assumed. Therefore, the upper limit for the contribution of homogeneous chemistry to the night-time ozone loss rates in the upper part of the PBL is of the order of 5 ppb, i.e. 25% of the observed ozone loss rates (Table 1). Thus homogeneous chemistry is only partially responsible for the observed ozone decrease, and further processes (others than large-scale horizontal transport and turbulent exchange) must be taken into consideration.

3.2.2.2. Temperature. Analysing the temperature data is somewhat difficult, since for some days in late evening, short-time advection of warm air was of some importance. These short-time processes result in an increase of the temperature after sunset, and its influence can therefore easily be recognized (see also Subsection 3.2.1). The effects of these processes can even be seen in the averaged data of periods 2, 3 and 4, due to the fact that the short-time disturbances occurred during the same time interval for several days. Thus for periods 2 to 4, the cooling rates during the first part of the night are lower than for the period after midnight (Table 2).

Apart from transport, the only mechanisms which contribute to the cooling of the air within the PBL are radiational processes due to the occurrence of water vapour, carbon dioxide, ozone and aerosols. Estimates of the influence of these processes were obtained using the Elsasser radiation chart (Charney, 1945; Elsasser and Culbertson, 1960; Zdunkowski et al., 1966) as well as results from a variety of studies (Grassl, 1973; Welch and Zdunkowski, 1976; Yueh and Chameides, 1979; André and Mahrt, 1982). The cooling rates computed on the basis of the diagram are given in Table 2 (theoretical values). From these studies, it can be concluded that the aerosols contribute much less to the long-wave radiational cooling rates than the trace gases, particularly water vapour. In relation to our measurements, which – although indicating a certain man-made influence – do not show a heavily polluted situation, it can be assumed that the maximum cooling rate due to aerosol-effects is approximately 0.05 K/h. Thus with the theoretical values of Table 2, an upper limit of 0.2 K/h for the total radiational cooling rate results. A comparison with the measurements shows that with the exception of the first part of the nights of the periods 2 to 4 (which show the influence of short-time disturbances), all values clearly exceed the theoretically estimated upper limit for radiational cooling effects (Table 2). Since large scale advective influence can be neglected and turbulence is ineffective, in addition to radiational cooling a further process affecting the temperature daily variation must exist in our topography.

3.2.2.3. Humidity. There is no source of water vapour at this height interval and furthermore no indications for strong large-scale advective influence exist. Thus, the increase in the water vapour mixing ratio must be attributed to some transport processes not mentioned as yet. From Figs. 6 and 7, one could infer that a very systematically

Table 2. *Cooling rates (K/h) in the layer between 400 and 800 m above Merenschwand for periods 1 to 4*

	Measurements						Theoretical values		
Period	18–20	20–22	22–24	24–02	02–04	04–06	2300	0100	0300
1	0.50	0.41	0.40	0.54	0.51	0.48	0.14	0.12	0.13
2	−0.04	0.01	0.40	0.34	0.38	0.26	0.12	0.11	0.12
3	−0.13	0.12	0.01	0.39	0.56	0.35	0.13	0.14	0.15
4	0.09	0.14	0.17	0.30	0.49	0.31	0.13	0.15	0.15

Measured values are averaged rates for the indicated time periods (LST). Theoretical values are inferred from the Elsasser diagram by using temperature and humidity data from ascents at the indicated time (LST).

occurring process has given rise to the distinct daily variation of humidity.

3.2.2.4. General features. The night-time decrease in the ozone content and temperature are partially attributable to homogeneous chemistry and radiational cooling, respectively. However, the increase in humidity can only be the result of a transport mechanism, which is neither large-scale horizontal advection nor turbulent transport. In addition, this mechanism should preferably be associated with a decrease in ozone and temperature. It is only the earth's surface that can in effect act as a source of water vapour and sink for ozone and temperature at the same time. Hence we shall assume a transport process which results in a coupling between the processes near the ground and those in the upper part of the PBL.

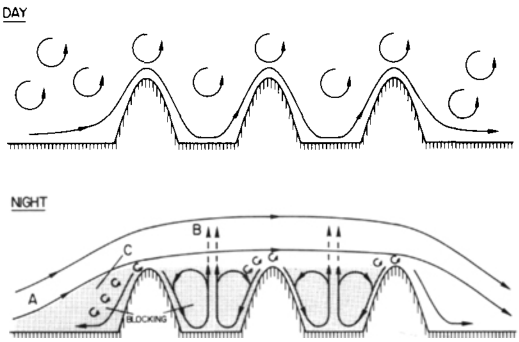

Fig. 9. Schematic representation of topography-induced transport processes in a regional scale of the Swiss Plateau. (For discussion of processes A, B and C, see text.)

3.2.3. Transport processes due to non-homogeneity of terrain

A strong coupling between the ground based processes and those at higher levels can be generated by a periodic change in the wind field, which occurs due to the phenomenon of blocking. In the following, we shall discuss whether the change in the characteristics of the wind field between day (no blocking) and night (blocking) has given rise to the observed effects.

The daytime PBL in flat as well as hilly terrain is dominated by turbulent transport, and the vertical gradients of potential temperature and water vapour mixing ratio nearly vanish. The earth's ground and its plant cover act as a source of heat and humidity for the boundary layer. Due to photochemical activities, an efficient production of ozone is to be expected. This production is partially compensated for by ozone destruction at the ground, i.e. dry deposition. At the upper boundary of the mixing layer in turn, air with a low ozone content is mixed down. This air is also very dry, therefore the increase in the humidity content remains limited, or even a decrease of humidity can be observed (Figs. 6 and 7). Thus, the layers above and below the ridge line undergo a strong coupling and the processes at the lower and upper boundaries have comparable effects to the air in both height intervals (Fig. 9).

After sunset, a drastic change in the efficiency of several processes occurs. The ozone production vanishes and the ozone content near the ground diminishes due to the combined effects of dry deposition, homogeneous chemistry and turbulent just as local induced transport. Furthermore the ground is acting as a source for water vapour, since the water vapour release by the plants does not cease fully during night-time (Rutter, 1975). If transport processes (e.g. within layers of downslope winds) prevent the occurrence of stagnant air masses near the ground, the efficiency of water vapour release to the air remains large, since no condensation is to be expected. Thus a further increase in the humidity content may be observed and additionally the temperature drops, due to the ground acting as a sink for heat.

For the analysis of the transport effects, we firstly assume that no blocking could be observed. Then the air masses would be transported along terrain-following streamlines. Thus air, which once has been close to the ground would always remain near to the surface and no coupling between the processes at the ground and those in the layers above crest height could be observed (Fig. 9, Streamlines like during the day). This situation is completely different if blocked air masses exist as in our case (cf. section 3). Then the air, which has been near to the ground somewhere in the surrounding regions, is transported across our valley at levels above the crest height (Fig. 9, Streamlines indicated by A). Thus the effects of processes near the ground can also be observed at the upper levels. However, it must be mentioned that the efficiency of this coupling decreases with growing night-time cooling, since the cold air masses near the ground are increasingly blocked on the windward side of the hills. A comparable effect arises due to the occurrence of blocked air masses in the neighbouring valleys of our measuring site.

Thus further transport processes must exist, which give rise to an additional coupling between the lower and the upper part of the PBL. The first of these processes occurs due to the influence of local wind systems in the neighbouring valleys. We must conclude that a local wind system comparable to that of the Reuss valley also occurs in these areas. As discussed earlier, under such conditions, a certain part of the air in the layers above crest height is continuously replaced by air from below due to the upward flow induced by the local wind system (cf. Subsection 3.2). Considering exclusively the Reuss valley, it was concluded that the observations in the upper layers could not be explained by the effects of this process alone. However, if such processes also occur in the neighbourhood, the effects are cumulative, when the air is transported across the different valleys (Fig. 9, process indicated by B). Therefore, this compensates to some extent for the decreasing effects arising from the periodic change in the flow characteristics. A further process which gives rise to the observed coupling, was first discussed by Yamada (1983). His model results show that on the windward side of a two-dimensional hill, zones with very efficient turbulent exchange exist. The zones occur due to the interaction between the mean wind field and the downslope winds, leading to the occurrence of recirculation phenomena. It seems reasonable to assume that comparable processes can also be encountered in our measuring area (Fig. 9, process indicated by C).

Thus, under the influence of the last-mentioned two processes, the efficiency of the coupling between the lower and the upper part of the PBL is maintained and in consequence, our observations show relatively cold, ozone-weak and water-vapour-rich air at levels above the crest during the whole night.

4. Conclusions

An analysis of the night-time variation of ozone, humidity and temperature in the layers of the PBL above the crest height of the ridge-valley system of our field experiment leads to the conclusion that several mechanisms affect the behaviour of these parameters. Homogeneous chemistry contributes to the night-time ozone loss, and radiational cooling to the temperature decrease. Both of these parameters, in addition to humidity, show a strong response to ground processes. The coupling is due to transport processes, which are in turn the result of the orographic forcing of the mean wind field and the interaction of mean flow with locally induced wind systems. Thus, the observations for the upper part of the PBL cannot be explained entirely by local effects. An additional influence due to the complex topography on a more regional scale is also felt.

The resultant atmospheric structure shows large deviations from the observed structure of the upper part of the PBL above flat terrain. This implies that increased efforts should be made to allow for this non-linear interaction between the large-scale wind field and terrain-induced phenomena when assessing the air quality situation as well as when making regulatory applications of air pollution models. In addition, further experimental research is needed for an integral understanding of the specific processes occurring in the PBL over nonhomogeneous terrain.

5. Acknowledgments

We wish to thank Professor H. U. Dütsch and Professor H. C. Davies for many valuable discussions. This research was supported by the Swiss National Science Foundation, the Swiss Federal Institute of Technology (ETH) and the Federal Office for Education and Science (COST 61a bis).

6. Appendix A

In order to evaluate the defining equation of the Froude number (cf. eq. 1)

$$\mathrm{Fr} = \bar{u}/N \cdot H \tag{A1}$$

for field data, the computing procedure must be specified. In our situation, the temperature measurements in the layer 200–600 m AGL and the wind data in 400–600 m AGL were assumed to be representative for the upstream flow situation in the PBL. (A sensitivity analysis showed that Fr is scarcely influenced by the choice of the height intervals.) Therefore N and $\bar{u}$ were calculated as

Table A1. Froude-numbers for the 4 averaging periods at the indicated time (LST)

Period	16	18	20	22	24	02	04	06	08	10	12	14
1	>10	>10	4.5	0.4	0.4	0.5	0.6	0.4	0.3	3.5	>10	>10
2	>10	>10	2.9	0.7	0.4	0.3	0.3	0.4	0.5	0.7	2.3	>10
3	>10	1.6	0.6	0.6	0.6	0.5	0.3	0.3	0.3	0.4	0.4	>10
4	>10	4.7	1.2	0.7	0.6	0.5	0.4	0.4	0.3	0.3	1.6	>10

bulk respective mean values in the respective height intervals:

$$N^2 = \frac{g \cdot [\theta(600\text{ m}) - \theta(200\text{ m})]}{\theta(400\text{ m}) \cdot 400\text{ m}}, \tag{A2}$$

$$\bar{u} = [u(600\text{ m}) + u(500\text{ m}) + u(400\text{ m})]/3. \tag{A3}$$

The Froude-numbers given in Table A1 for the 4 periods are computed by averaging the values of Fr of the single days.

7. Appendix B

The Richardson-number Ri is evaluated over 50 m layers as proposed by Mahrt et al. (1982). In particular,

$$\mathrm{Ri} = \frac{g \cdot \Delta\theta \cdot 50\text{ m}}{\theta_0 \cdot (\Delta u^2 + \Delta v^2)}, \tag{B1}$$

where $\Delta\theta$, Δu and Δv are the changes of potential temperature and wind components across 50 m layers.

Table B1. Richardson-numbers for the 4 averaging periods at the indicated time (LST)

Period	Height (m AGL)	20	22	24	02	04	06
1	500	0.1	3.5	2.3	2.2	1.6	1.0
	700	−0.1	2.5	2.3	2.2	3.2	3.9
2	500	0.2	0.5	0.7	3.1	3.2	5.0
	700	1.1	1.5	1.3	3.1	3.4	2.1
3	500	−0.7	2.8	1.6	1.2	2.1	3.8
	700	1.7	2.5	2.1	3.9	5.2	8.2
4	500	−0.7	1.9	2.8	1.6	1.6	2.0
	700	3.0	4.0	4.2	3.0	3.8	4.9

Table B1 presents values of Ri for the height of 500 m and 700 m AGL between 2000 LST and 0600 LST. The Ri-numbers for the 4 periods are calculated by averaging the values of Ri for the single days.

REFERENCES

André, J. C. and Mahrt, L. 1982. The nocturnal surface inversion and influence of clear-air radiative cooling. *J. Atmos. Sci. 39*, 864–878.

Bell, R. C. and Thompson, R. 1980. Valley ventilation by cross winds. *J. Fluid. Mech. 96*, 757–767.

Broder, B. and Gygax, H. A. 1985. The influence of locally induced wind systems on the effectiveness of nocturnal dry deposition of ozone. *Atm. Environ.* in press.

Charney, J. 1945. Radiation. In: *Handbook of meteorology*, ed. F. A. Berry, E. Bollay and N. R. Beers. McGraw-Hill, New York.

Elsasser, W. M. and Culbertson, M. F. 1960. Atmospheric radiation tables. *Meteorol. Monogr. 23*. American Meteorological Society.

Grassl, H. 1973. Aerosol influence on radiative cooling. *Tellus 25*, 386–395.

Gygax, H. A., Broder, B. and Tinguely, M. 1985. Planetary boundary layer measurements over non-homogeneous terrain: data of the Reuss-valley experiment 1982. *Publ. Atmospheric Physics*, Swiss Federal Institute of Technology, *LAPETH-26*.

Kondo, J., Kanechika, O. and Yasuda, N. 1978. Heat and momentum transfers under strong stability in the atmospheric surface layer. *J. Atmos. Sci. 35*, 1012–1021.

Mahrt, L., André, J. C. and Heald, R. C. 1982. On the depth of the nocturnal boundary layer. *J. Appl. Meteorol. 21*, 90–92.

Manins, P. C. and Sawford, B. L. 1982. Mesoscale observations of upstream blocking. *Q. J. R. Meteorol. Soc. 108*, 427–434.

Platt, U., Perner, D., Schroeder, S., Kessler, C. and

Toennissen, A. 1981. The diurnal variation of NO_3. *J. Geophys. Res. 86*, 11965–11970.

Rutter, A. J. 1975. The hydrological cycle in vegetation. In: Monteith, J. L. (ed.): *Vegetation and the atmosphere*. Vol. 1, Principles. Academic Press, London, 111–154.

Welch, R. and Zdunkowski, W. 1976. A radiation model of the polluted atmospheric boundary layer. *J. Atmos. Sci. 33*, 2170–2184.

Yamada, T. 1983. Simulations of nocturnal drainage flows by a $q^2 l$ turbulence model. *J. Atmos. Sci. 40*, 91–106.

Yueh, W. R. and Chameides, W. L. 1979. A perturbative treatment of aerosol scattering of infrared radiation. *J. Atmos. Sci. 36*, 1997–2005.

Zdunkowski, W. G., Barth, R. E. and Lombardo, F. A. 1966. Discussion on the atmospheric radiation tables by Elsasser and Culbertson. *Pure Appl. Geophys. 63*, 211–219.